

The study of colliding vortex rings using a special-purpose computer and FMM*

Tarun Kumar SHEEL¹, Rio YOKOTA¹, Kenji YASUOKA², and Shinnosuke OBI²

¹ Graduate School of Science and Technology, Keio University

² Department of Mechanical Engineering, Keio University
(3-14-1 Hiyoshi, Kouhoku-ku, Yokohama, 223-8522, Japan)

The present study involves a novel numerical technique regarding the simultaneous use of the fast multipole method (FMM) and a special-purpose computer originally designed for molecular dynamics simulations (MDGRAPE-3). In the present calculations, the dynamics of two colliding vortex rings have been studied using the vortex method and the computation time has been reduced by a factor of 2000 compared to a direct calculation on a standard PC. The reconnection of the vortex rings was clearly observed, and the discretization error became nearly negligible for the calculation using 10^7 elements.

Key Words: Vortex Method, Vortex Dynamics, Fast Multipole Method, Special-Purpose Computer

1. Introduction

There has always been a strong relation between the progress in vortex methods and advancements of the acceleration techniques, which the vortex method uses. When the classical vortex methods became popular nearly 30 years ago, the calculation cost of the N-body solver was $O(N^2)$, where N is the number of particles to be calculated. Due to this enormous calculation cost, the intention at that time was not to fully resolve the high Reynolds number fluid flow, but to somewhat mimic the dominant vortex dynamics using discrete vortex elements.

The application of fast N-body solvers enabled the calculation of millions of vortex elements⁽¹⁾. The fast algorithms were also applied to the boundary integral calculations⁽²⁾. Furthermore, fast N-body solvers were not only used for vortex particle methods, but also vortex tube methods⁽³⁾. These efforts led to a new paradigm, i.e. solving flows of moderate Reynolds numbers and fully resolving these flows.

However, the high proportionality constant of the fast

N-body solvers prevented them from matching the speed of grid based fast Poisson solvers. Since the mainstream methods in computational fluid dynamics use fast Poisson solvers, it was still difficult for vortex methods to be considered as an alternative to conventional grid based methods.

The shortcomings of the fast N-body solvers can partly be circumvented by the use of hybrid methods, while the Lagrangian nature of the convection calculation is retained. The vortex-in-cell is a typical hybrid method, and its accuracy and speed are quite close to that of the spectral method⁽⁴⁾. The particle-mesh method is another hybrid approach. Sbalzarini et al.⁽⁵⁾ developed a particle-mesh library that calculates one vortex method iteration for 268 million particles in 85 seconds using 128 processors. This is comparable to the performance of the state-of-the-art finite difference methods using processors of comparable performance.

Another way to fill the gap between the N-body solver and fast Poisson solver is to use a hardware specialized for N-body calculations, such as the MDGRAPE-3⁽⁶⁾. Ever since the GRAPE⁽⁷⁾ was first introduced, these special purpose computers have constantly outperformed the general purpose computers of the same price.⁽⁶⁾ The special-purpose computers can also be used for the boundary integral calculation.⁽⁸⁾ At this point, it is not yet evident which will prevail: Fast Poisson solvers on par-

* 原稿受付 2007 年 12 月 07 日, 改訂 2007 年 12 月 28 日, 発行 2008 年 02 月 04 日. ©2008 日本計算工学会.

Manuscript received, December 07, 2007; final revision, December 28, 2007; published, February 04, 2008. Copyright ©2008 by the Japan Society for Computational Engineering and Science.

allel general purpose architecture, or fast N-body solvers on parallel special purpose processors. In our present study, we will investigate the possibility of accelerating the direct summation part of the fast multipole method (FMM) by Cheng et al.⁽⁹⁾ using a special purpose hardware; MDGRAPE-3.

We choose the collision of vortex rings as a test case. The following characteristics of this flow allow us to focus on the assessment of the present acceleration technique. The flow does not involve solid or periodic boundaries, thus causes minimum complication in the implementation of the FMM itself. Also, the initial condition is simple to generate for vortex methods. Furthermore, although the initial flow field is quite simple, the collision of the rings results in a highly turbulent state, and the mixing process is strongly affected by the Reynolds number. This allows us to assess the ability of vortex methods to handle high Reynolds number flows by using a large number of particles, which becomes possible with the use of the present acceleration method.

We first discuss the efficient implementation of the FMM on the MDGRAPE-3. Then we apply our method to the vortex method calculation of colliding vortex rings. The effect of spatial resolution at high Reynolds numbers is investigated by comparing the energy spectrum and decay rate of the kinetic energy.

2. Numerical Methods

2.1 Vortex Method The vortex method describes the flow field by the superposition of particles with a smooth distribution of vorticity.⁽¹⁰⁾ From this vorticity, the velocity of vortex elements is calculated by the Biot-Savart equation. The vortex elements are then convected according to this velocity, and at the same time, the vorticity is updated according to the stretching and diffusion term of the vorticity equation. We will only show the final discretized form of each equation here.

The discretized form of the Biot-Savart equation with algebraic cutoff function by Winkelmanns et al.⁽¹¹⁾ calculates the velocity \mathbf{u} of a vortex element by

$$\mathbf{u}_i = -\frac{1}{4\pi} \sum_{j=1}^N \frac{|\mathbf{r}_{ij}|^2 + (5/2)\sigma_j^2}{(|\mathbf{r}_{ij}|^2 + \sigma_j^2)^{5/2}} \mathbf{r}_{ij} \times \boldsymbol{\gamma}_j \quad (1)$$

The subscript i stands for the target elements, while j stands for the source elements, thus $\mathbf{r}_{ij} = \mathbf{x}_i - \mathbf{x}_j$ is the distance vector. $\boldsymbol{\gamma}$ is the vortex strength and σ is the core radius of the vortex element.

Using the same algebraic function as above, the stretch-

ing term becomes⁽¹¹⁾

$$\frac{d\boldsymbol{\gamma}_i}{dt} = \frac{1}{4\pi} \sum_{j=1}^N \left\{ -\frac{|\mathbf{r}_{ij}|^2 + (5/2)\sigma_j^2}{(|\mathbf{r}_{ij}|^2 + \sigma_j^2)^{5/2}} \boldsymbol{\gamma}_i \times \boldsymbol{\gamma}_j + 3 \frac{|\mathbf{r}_{ij}|^2 + (7/2)\sigma_j^2}{(|\mathbf{r}_{ij}|^2 + \sigma_j^2)^{7/2}} (\boldsymbol{\gamma}_i \cdot (\mathbf{r}_{ij} \times \boldsymbol{\gamma}_j)) \mathbf{r}_{ij} \right\} \quad (2)$$

For the calculation of the diffusion term, we use the core spreading method⁽¹²⁾, which uses the relation

$$\frac{d\sigma_i}{dt} = \frac{\nu}{\sigma_i} \quad (3)$$

The radial basis function interpolation⁽¹³⁾ is used every ten time steps to ensure the convergence of the core spreading method.⁽¹⁴⁾ The convection is solved by updating the position of vortex elements according to their velocity

$$\frac{d\mathbf{x}_i}{dt} = \mathbf{u}_i \quad (4)$$

In summary, the vortex method sequentially solves Eqs. (1), (2), (3), and (4). The MDGRAPE-3 and FMM are used to calculate Eqs. (1) and (2).

2.2 MDGRAPE-3 The MDGRAPE-3 is a special-purpose computer exclusively designed for molecular dynamics simulations. A typical MDGRAPE-3 system consists of a general-purpose computer and a special-purpose hardware connected via a PCI board. The MDGRAPE chips can only handle two types of calculations. The Coulomb potential

$$p_i = \sum_{j=1}^N b_j g(a|\mathbf{r}_{ij}|^2), \quad (5)$$

and Coulomb force

$$\mathbf{f}_i = \sum_{j=1}^N b_j g(a|\mathbf{r}_{ij}|^2) \mathbf{r}_{ij}. \quad (6)$$

$g()$ is an arbitrary function, which must be defined prior to the calculation. a and b_j are constants, which can be used for scaling. The direct form of the Biot-Savart equation (1) and the stretching term (2) can be calculated by using a combination of (5) and (6).

The function $g()$ for an arbitrary value $a|\mathbf{r}_{ij}|^2$ is calculated by interpolation, from values that are tabulated prior to the execution of the main program. If the interparticle distance is such that $a|\mathbf{r}_{ij}|^2$ falls out of this tabulated domain, the MDGRAPE assumes $g()$ is zero. The number of tabulated points is constant, thus defining the table in a large domain would result in larger spacing between the tabulated points, and therefore larger interpolation error. Contrary, defining the table in a small domain would yield a higher possibility of the interparticle spacing falling outside the tabulated domain, which also causes error.

The three critical issues regarding the implementation of the MDGRAPE on vortex methods are the efficient calculation of the Biot-Savart and stretching equation, the optimization of the table domain, and the minimization of the round-off error caused by the partially single precision calculation in the MDGRAPE. These problems were investigated by Sheel et al.⁽¹⁵⁾ for the preceding but similar machine; MDGRAPE-2. The only difference between the MDGRAPE-2 and MDGRAPE-3 is that the latter can simultaneously calculate along with the host machine, but can only handle a small number of source particles at once.⁽⁶⁾ However, these differences do not have any effect on the above mentioned critical issues, and the findings of Sheel et al.⁽¹⁵⁾ can be directly used for the MDGRAPE-3.

2.3 FMM on MDGRAPE-3 The most important issue regarding the simultaneous use of the FMM and MDGRAPE-3 is the balance of the workload between the multipole to local translation and the direct summation. Only the latter can be handled by the MDGRAPE-3, hence it is necessary to optimize the level of box divisions according to the computer load in order to achieve the best performance of acceleration.

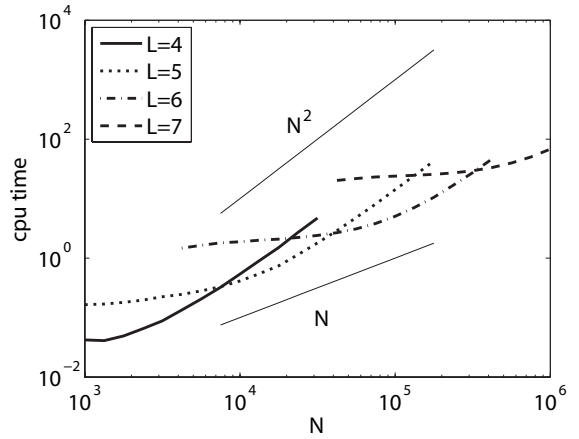
We will now investigate the optimum load balance for the FMM with and without the MDGRAPE-3. The CPU-time of the Biot-Savart calculation is plotted against the number of elements for different box levels and shown in Fig. 1. L is the level of the oct-tree box division, where the original domain is divided into $2^L \times 2^L \times 2^L$ boxes. The details of our FMM follow that of Cheng et al.⁽⁹⁾ The order of multipole expansion is $p = 10$ for all calculations.

Fig. 1(a) shows that when N is increased from 10^3 to 10^6 , the optimum box division level of the FMM gradually increases from $L = 4$ to $L = 7$. When the FMM is used with the MDGRAPE-3, the balance changes significantly due to the acceleration of the direct summation, as shown in Fig. 1(b).

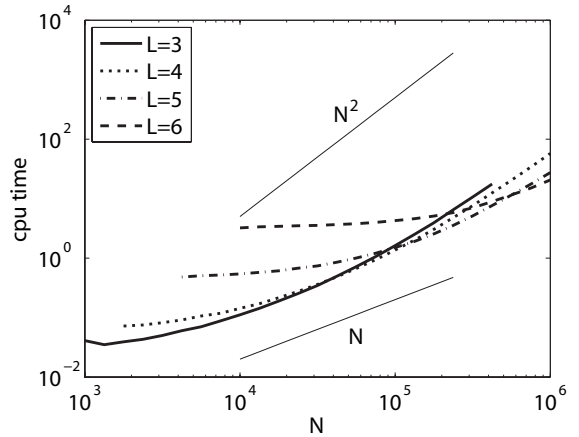
In summary, the optimum level of box division of the FMM on the MDGRAPE-3 is approximately two levels lower than that of the FMM without the MDGRAPE-3 because only the direct summation is accelerated.

2.4 Test for CPU-time and Error The CPU-time and error of the FMM and MDGRAPE-3 are tested by a combinatorial comparison of the calculations with and without them. The testing conditions are summarized in Table 1. "Xeon" refers to the calculations performed on a dual core Xeon 5160 (3.0GHz) processor.

The CPU-time for all cases (when optimized) are compared in Fig. 2. Case 1 has a high constant and is of the order $O(N^2)$. Case 2 has a lower constant but is still proportional to $O(N^2)$. Conversely, Case 3 has



(a) FMM



(b) FMM-MDG3

Fig.1 Change in optimum box level for different methods

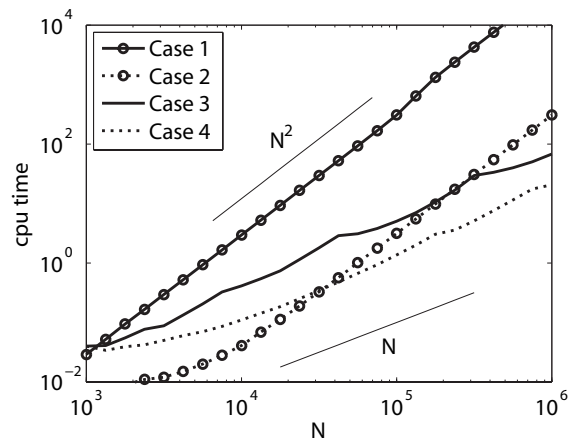


Fig.2 CPU-time of different methods

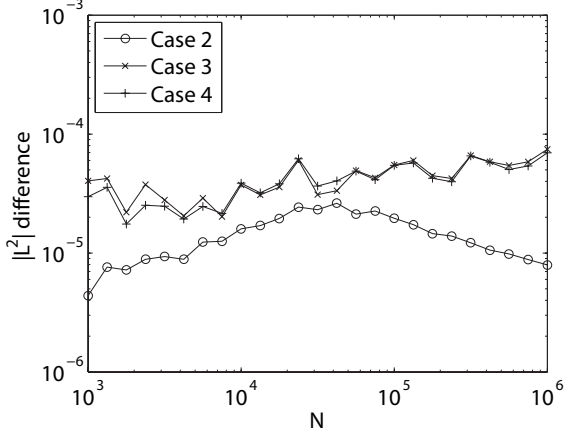


Fig.3 $|L^2|$ of different methods

Table 1 Combination of the testing conditions

	Xeon	MDGRAPE-3
Direct Calculation	Case 1	Case 2
FMM	Case 3	Case 4

a high constant but the order is $O(N)$. Case 4 has a low constant and is of order $O(N)$. At $N = 10^6$ the FMM on MDGRAPE-3 is about 16 times faster than the MDGRAPE-3 itself, and approximately 4 times faster than the FMM on the Xeon, see Fig. 2.

The L^2 norm of the difference relative to Case 1 is shown in Fig. 3. The MDGRAPE-3 contains errors of its own, which stem from the partially single precision calculation, and use of interpolation during the calculation of the table function as already found by Sheel et al.⁽¹⁵⁾ This error is constantly lower than the FMM errors for $10^3 \leq N \leq 10^6$. The errors of the FMM are also significantly lower than the errors in the vortex method itself, which are on the order of 10^{-3} .

It is concluded that, the approximation error of the FMM, and the round-off error of the MDGRAPE-3 are significantly small compared to the discretization error of the vortex method. Hence, the use of the present acceleration method is effective for the vortex method calculation.

3. Vortex Ring Calculation

3.1 Calculation Condition The initial radius of the vortex rings was $R = 1$ while the cross-section radius was $r = 0.05$, see Fig. 4. The rings were inclined at an angle $\theta = 15^\circ$ relative to the z -axis. The Reynolds number based on the ring circulation was $Re_\Gamma = \Gamma/\nu = 400$.

Two types of initial conditions were used for the present investigation. The first was identical to our previous

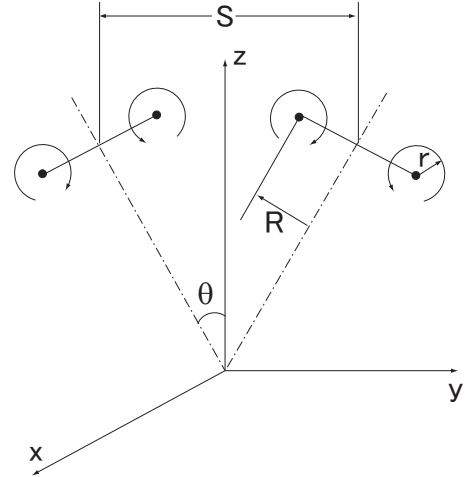


Fig.4 Initial position of rings

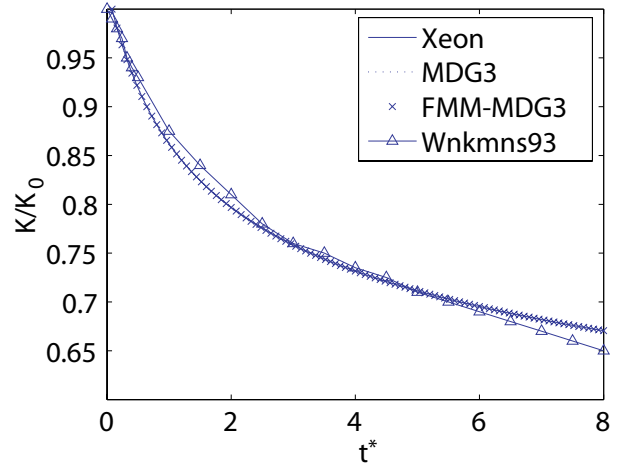


Fig.5 Time history of kinetic energy

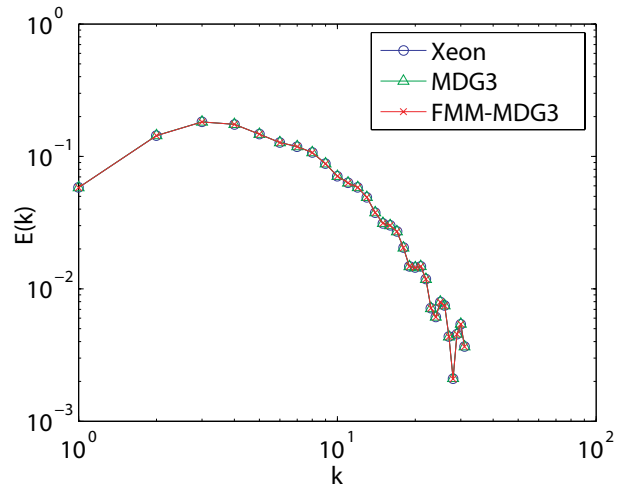


Fig.6 Energy spectra

calculations,⁽¹⁵⁾ which was used to validate our present method by reproducing previous results. For this case, the initial core radius of the vortex elements was $\sigma_0 = 0.065$, and the total number of elements was $N \approx 6 \times 10^4$, with the number of cross sections in the circumference direction being 502, while 61 elements were distributed in each cross-section of the two rings. The absolute value of the vortex strength was constant for all elements.

In the second condition, the initial condition was modified so that the vortex method could stably calculate until the reconnection occurred. This second initial condition had a Gaussian distribution of vorticity in the cross section, as observed in experiments.⁽¹⁶⁾ The vortex elements were distributed up to $3\sigma_g$, where σ_g is the standard deviation of the Gaussian distribution. This allows the diffusion to take place at the regions surrounding the vortex ring. Furthermore, the initial core radius of the vortex elements σ_0 was set to twice the inter-particle spacing, which guarantees the overlap of elements for long calculations.

3.2 Comparison with Previous Calculations

The collision of vortex rings is calculated using the first condition mentioned above. The kinetic energy K is evaluated by the same method used in Winckelmans et al.⁽¹¹⁾ The evolution of the kinetic energy is compared with that of Winckelmans et al.⁽¹¹⁾ in Fig. 5. The time $t^* = t\Gamma/R^2$ is used hereafter, which is normalized by the circulation and radius of the vortex ring. The kinetic energy is normalized by its initial value. The Xeon, MDG3, FMM-MDG3, and Wnkms93, represent the direct calculation on the Xeon, direct calculation on the MDGRAPE-3, the FMM on the MDGRAPE-3, and the results of Winckelmans et al.⁽¹¹⁾ The difference between the present calculation and the results of Winckelmans et al.⁽¹¹⁾ is marginal. The energy spectra are calculated from the velocity distribution along the z -axis at selected times, and shown in Fig. 6. The results with and without the FMM do not show any notable difference.

3.3 Calculation with Improved Initial Conditions

The collision of vortex rings is calculated using the second condition. The number of particles is changed for $10^5 \leq N \leq 10^7$, while the Reynolds number is kept constant. The corresponding number of elements per cross section and number of cross sections are shown in Table 2. These numbers are determined by choosing a inter-particle distance that yields the total number of elements closest to $N \approx 10^5$, $N \approx 10^6$, and $N \approx 10^7$.

The movement of vortex elements for Case A, is illustrated in Fig. 7. At (a) $t^* = 15$, the two rings collide and begin to merge. At (b) $t^* = 30$, the two rings merge into one. At (c) $t^* = 45$ the vortex rings reconnect and form two new rings. One of the key features

Table 2 Breakdown of the Number of Elements

Case	A	B	C
Number of Rings	2	2	2
N per Cross Section	190	418	910
Cross Sections	271	1261	5677
Total	102980	1054196	10332140

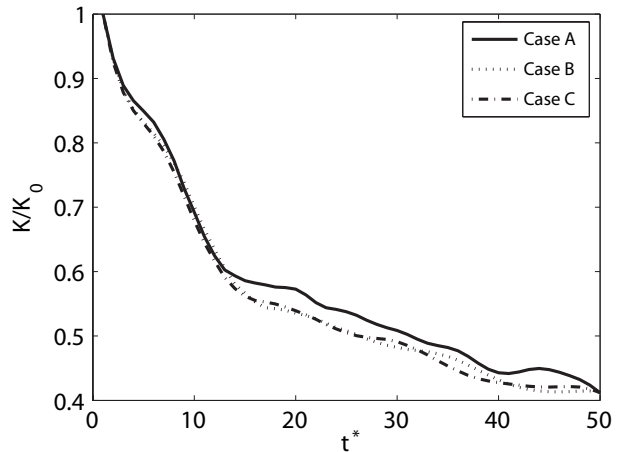


Fig. 8 Effect of spatial resolution on the decay of kinetic energy

of the present calculation is that the vortex reconnection is reproduced more realistically than the previous calculations by Winckelmans et al.⁽¹¹⁾ and Fukuda & Kamemoto⁽¹⁷⁾. These results are supported by the fact that the present method can handle the diffusion more accurately since it considers the diffusion in the region surrounding the rings and also uses an accurate spatial adaption technique to ensure the convergence of the diffusion scheme for longer calculations. The reconnection observed here is also similar to the DNS results of Cottet & Koumoutsakos⁽¹⁰⁾ and experimental results by Kida et al.⁽¹⁸⁾.

3.4 Effect of Spatial Resolution

We will now show the necessity of a large number of particles to reproduce the quantitative aspects of the flow. The kinetic energy $K = 1/2u_i^2$ is calculated from the velocity of the vortex elements directly. The decay of kinetic energy are shown in Fig. 8 to compare the results for different N . A quantitative difference between Case A and the other two is clearly observed. Thus, as the number of elements is increased from $N \approx 10^5$ to $N \approx 10^7$, the energy decay shows convergent behavior with respect to N .

The energy spectra are calculated from the velocity distribution along the z -axis at selected times. The energy spectrum is shown in Fig. 9. The transfer and dis-

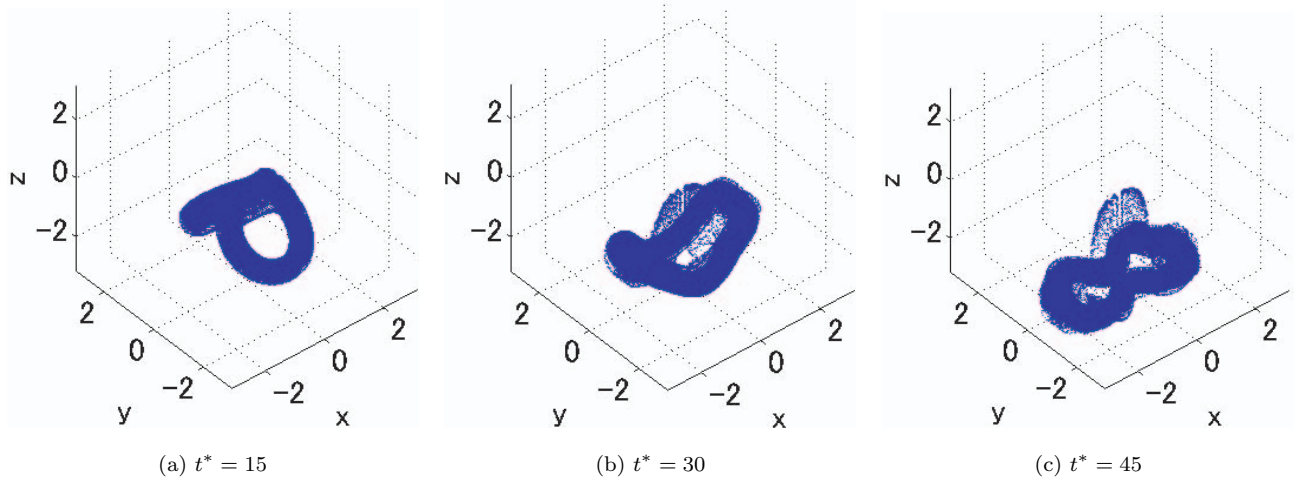


Fig.7 Position of vortex elements for Case A

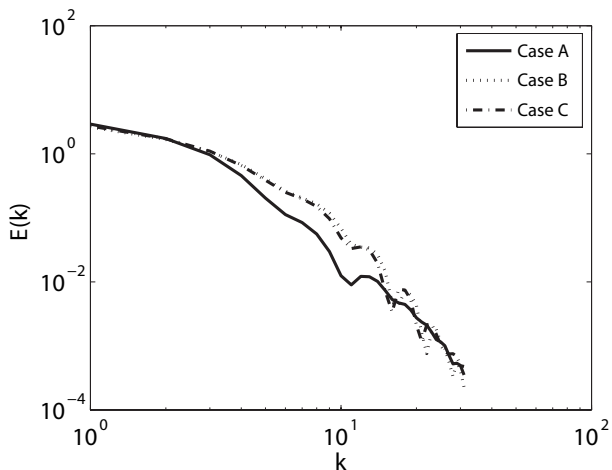


Fig.9 Effect of spatial resolution on the energy spectra at $t^* = 45$

sipation of kinetic energy determines the shape of the energy spectrum. Therefore, the agreement of the energy spectra reflects the soundness of the transfer and dissipation calculation. It is seen from Fig. 9 that the energy spectra match when $N \geq 10^6$.

In summary, the number of elements required to accurately predict the transfer and dissipation of kinetic energy is $N \geq 10^6$ for the present Reynolds number $Re_\Gamma = 400$.

4. Conclusions

The vortex method calculation is accelerated by the simultaneous use of the FMM and a special purpose computer MDGRAPE-3. The FMM on MDGRAPE-3 is about 16 times faster than the MDGRAPE-3 itself, and approximately 4 times faster than the FMM on a Xeon 5160 (3.0 GHz) for the Biot-Savart calculation of $N = 10^6$ elements. The errors involved in the use of the MDGRAPE-

3 are less than the errors of the FMM, and thus are small enough to perform an accurate vortex method calculation.

The collision of two vortex rings is selected as a test case. The reconnection of the vortex rings in the present calculation is similar to what is seen in experimental and DNS results. This is a result of the high precision of the stretching and diffusion calculations. The results of the calculations using more than 10^6 particles, not only reproduce the qualitative aspects of the reconnection, but also show nearly negligible discretization error. These features support the use of pure Lagrangian vortex methods in fairly complex 3-D flows.

5. Acknowledgements

We are grateful to Dr. T. Narumi (Keio University, Japan) for his support to develop the MDGRAPE-3 and valuable suggestions upon using it.

References

- (1) Salmon, J. K. and Warren, M. S., Fast Parallel Tree Codes for Gravitational and Fluid Dynamical N-Body Problems *Int. J. High Perf. Comput. Appl.* Vol. 8, 1994, pp. 129–142.
- (2) Winckelmans, G. S., Salmon, J. K., Warren, M. S., Leonard, A., and Jodoin, B., Application of Fast Parallel and Sequential Tree Codes to Computing Three-Dimensional Flows with the Vortex Element and Boundary Element Methods, *ESAIM Proceedings*, Vol. 1, 1996, pp. 225–240.
- (3) Collins, J. P., Dimas, A. A., Bernard, P. S., A Parallel Adaptive Fast Multipole Method for High Performance Vortex Method Based Simulations, *Proc. ASME FED* Vol. 250, 1999.
- (4) Cottet, G. H., Michaux, B., Ossia, S., and VanderLinden, G., A Comparison of Spectral and Vor-

- tex Methods in Three-Dimensional Incompressible Flows, *J. Comput. Phys.* Vol. 175, 2002, pp. 702–712.
- (5) Sbalzarini, I. F., Walther, J. H., Bergdorf, M., Hieber, S. E., Kotsalis, E. M., and Koumoutsakos, P., PPM - A Highly Efficient Parallel Particle-Mesh Library for the Simulation of Continuum Systems, *J. Comput. Phys.* Vol. 215, 2006, pp. 566–588.
- (6) Narumi, T., Ohno, Y., Futatsugi, N., Okimoto, N., Suenaga, A., Yanai, R., and Taiji, M., A High-Speed Special-Purpose Computer for Molecular Dynamics Simulations: MDGRAPE-3, *Proceedings of NIC Workshop 2006*, Vol. 34, 2006, pp. 29–35.
- (7) Sugimoto, D., Chikada, Y., Makino, J., Ito, T., Ebisuzaki, T., and Umemura, M., A Special-Purpose Computer for Gravitational Many-Body Problems, *Nature* Vol. 345, 1990, pp. 33–35.
- (8) Takahashi, T., Kawai, A., and Ebisuzaki, T., Accelerating Boundary Integral Equation Method using a Special-purpose Computer, *Int. J. Numer. Meth. Eng.* Vol. 66, 2006, pp. 529–548.
- (9) Cheng, H., Greengard, L., and Rokhlin, V., A Fast Adaptive Multipole Algorithm in Three Dimensions, *J. Comput. Phys.* Vol.115, 1999, pp. 468–498.
- (10) Cottet G. H. and Koumoutsakos, P. D., *Vortex Methods* Cambridge University Press, pp. 245.
- (11) Winckelmans, G. S., Leonard, A., Contributions to Vortex Particle Methods for the Computation of Three-Dimensional Incompressible Unsteady Flows, *J. Comput. Phys.* Vol.109, 1993, pp. 247–273.
- (12) Leonard, A., Vortex Methods for Flow Simulations, *J. Comput. Phys.* Vol.37, 1980, pp. 289–335.
- (13) Barba, L. A., Leonard, A., and Allen, C. B., Advances in Viscous Vortex Methods- Meshless Spatial Adaption Based on Radial Basis Function Interpolation, *Int. J. Num. Meth. Fluids* Vol.47, 2005, pp. 387–421.
- (14) Yokota, R., Sheel, T. K., and Obi, S., Calculation of Isotropic Turbulence Using a Pure Lagrangian Vortex Method, *J. Comput. Phys.* Vol. 226, 2007, pp. 1589–1606.
- (15) Sheel, T. K., Yasuoka, K., and Obi, S., Fast Vortex Method Calculation Using a Special-Purpose Computer, *Comput. Fluids* Vol.36, 2007, pp. 1319–1326.
- (16) Shariff, K., Verzicco, R., and Orlandi, P., A Numerical Study of Three-Dimensional Vortex Ring Instabilities: Viscous Corrections and Early Non-linear Stage, *J. Fluid Mech.* Vol.279, 1994, pp. 351–375.
- (17) Fukuda, K. and Kamemoto, K. Application of a Redistribution Model Incorporated in a Vortex Method to Turbulent Flow Analysis, *Proc. 3rd Int. Conf. Vortex Flows Vortex Models, Yokohama, Japan 2005*, pp. 131–136.
- (18) Kida, S., Takaoka, M., Vortex Reconnection, *Annu. Rev. Fluid Mech.* Vol.26, 1994, pp. 169–189.